Crack Propagation Behavior Under Low-Cycle Corrosion Fatigue of A7003-T6 Aluminum Alloy*

Kazuaki SHIOZAWA**, Toru ASAMOTO***
and Kazyu MIYAO**

Crack propagation behavior has been observed in A 7003- T 6 aluminum alloy under low cyclic loading with hold time over the frequency range $4\times10^{-3}\sim1$ Hz in 3.0% saline solution. From the experimental results, the effect of cyclic frequency on crack propagation rates was found to be exemplified by two different regimes. One has a positive dependency on the frequency below a critical frequency, f_{crit}, at which point maximum environmental attack occurs in terms of da/dN, and the other is negative above f_{crit}. The behavior of crack propagation below f_{crit} was explained by the concept of stress-assisted dissolution which tends to inhibit mechanical failure by crack blunting and microbranching. The number and depth of secondary cracks occurring under the fracture surface were measured by metallographic examination, and the actual crack tip stress intensity factor was estimated.

Key Words: Corrosion Fatigue, Crack Propagation Rate, Aluminum Alloy, Secondary Crack, Frequency, Stress Waveform, Blunting, Branching

1. Introduction

Behavior of corrosion fatigue crack propagation is sensitively affected by the stress or strain waveform and loading frequency. The enhancement and retardation of the fatigue crack propagation rate due to the environment has recently received much attention[1]~[4]. It is generally acknowledged that crack propagation behavior under a low cyclic stress waveform is complex because of sensitivity to stress corrosion cracking, stress-assisted dissolution, crack blunting and microbranching at the crack tip.

Since crack propagation under a corrosive environment may be determined by the correlation of mechanical and electrochemical processes, it is convenient for the consideration of corrosion fatigue crack propagation to take into account the superposition of an environmental cracking component due to anodic dissolution and a pure mechanical fatigue component. Several researchers have attempted to combine these effects with simple models, based on macroscopic crack growth data, for example, the process superposition model proposed by Wei and Landes[5], the process competition model of Austen and Walker[6], and the process interaction model of Rhodes et al[7]. The relative contributions to crack propagation made by the electrochemical and mechanical cracking mechanisms obviously depend upon the frequency of applied load and loading waveform. These mechanisms may occur simultaneously and have mutual interactions during the low-cycle fatigue process. But the mechanisms of such interactions are not obvious because several specific interactions, in which one process may be inhibited or enhanced by the action of corrosive attack, are possible. This is the area of interest of the present investigation, since there is no satisfactory model to explain quantitatively the corrosion fatigue crack propagation effects. It is also noted that severe corrosion attack may cause blunting or microbranching of the crack tip.

As part of a series of studies on the influence of

* Received 10 th February, 1989. Paper No.87-1300 A
** Department of Mechanical Engineering, Faculty of Engineering, Toyama University, 3190 Gofuku, Toyama, 930, Japan
*** Nippon Kokan Light Steel Co., Ltd., Kumagaya, Saitama, 360, Japan

the interaction of stress cycling and stress corrosion on crack propagation, that is, cyclic stress corrosion cracking[8][9], we carried out a study including low cyclic corrosion fatigue tests of A 7003-T 6 aluminum alloy under triangular and trapezoidal waveforms, over the frequency range $4\times10^{-3}\sim1$ Hz in 3.0 % saline solution. Corrosion fatigue crack propagation rates were measured to determine the effect of frequency and waveform. The effect of corrosive attack on enhancement and retardation in crack propagation rates was considered in relation to experimental observations of blunting or microbranching of the crack tip.

2. Material and Testing Method

2.1 Material and specimen

The material examined in this study was a high-strength aluminum alloy, A 7003-T 6. It was supplied in rolled plates 10 mm thick. The alloy underwent the T 6 heat treatment solutionized at 773 K for 12 hours, quenched at 773 K for 2 hours, water cooled, and aged for 8 hours at 418 K. The chemical composition and room temperature mechanical properties are given in Tables 1 and 2.

Compact tension specimens with side grooves were machined to the dimensions shown in Fig. 1. The direction of crack propagation coincided with the rolling direction.

2.2 Testing method

Low-cycle fatigue tests were carried out using a specially designed testing apparatus driven by an electric motor constructed of a magnetic clutch, gear-box and warm gear. A servo-hydraulic fatigue machine was also used to obtain a high frequency range condition. The corrodent was 3.0% saline solution controlled at 298 ± 2 K and continuously circulated in a one-litre plastic reservoir through the cell at a flow rate of about 32 ml/min.

Crack extension was measured optically on the side face of the specimen by means of a traveling microscope with $\times100$ magnification directed through a glass window in the environmental chamber. The behavior of crack closure was monitored by the unloading elastic compliance technique using the back face strain gauge, as shown in Fig. 1.

Two types of stress waveform were used for most of the experiments. One was a triangular waveform, and the other, a trapezoidal waveform with hold time, t_h, and raise/fall time, t_c. The load ratio, R, of minimum load to the maximum load range was 0.1 in these experiments.

Table 1 Chemical composition of aluminum alloy.

(wt%)

Si	Fe	Cu	Mg	Mn	Zn	Zr	Ti	Al
0.07	0.17	0.15	0.82	0.02	5.74	0.15	0.01	Bal.

Table 2 Mechanical properties of material.

Yield strength $\sigma_{0.2}$ (MPa)	Tensile strength σ_B (MPa)	Elongation ε_f (%)
257	309	14.3

3. Experimental Results and Discussions

3.1 The effect of frequency and hold time on crack propagation

The experimental results for fatigue crack propagation rates in air and saline solution are shown in Fig. 2 for tests carried out at an R ratio of 0.1 with triangular and trapezoidal wave loading. All of the results followed well-established patterns. The saline solution data obtained from the triangular waveform at rise/fall time, t_c, from $1\sim250$ sec ($f=1\sim4\times10^{-3}$ Hz) are faster than those for the tests conducted in air ($f=1$ Hz), and there is an obvious effect of frequency on the fatigue crack propagation rate (Fig. 2(a)). Figure 2(b) shows the results obtained from the test condition of trapezoidal wave loading in which the load hold period, t_h, is changed from $5\sim500$ sec under a constant rise/fall time, t_c, of 10 or 45 sec. It is found from these results that the effect of hold periods on crack propagation rate is slight in trapezoidal wave loading.

From the experimental results of stress corrosion cracking in 3.0% saline solution conducted on the specimen described above, it was found that the value of K_{Iscc} is about 16.8 MPam$^{1/2}$, and that a plateau,

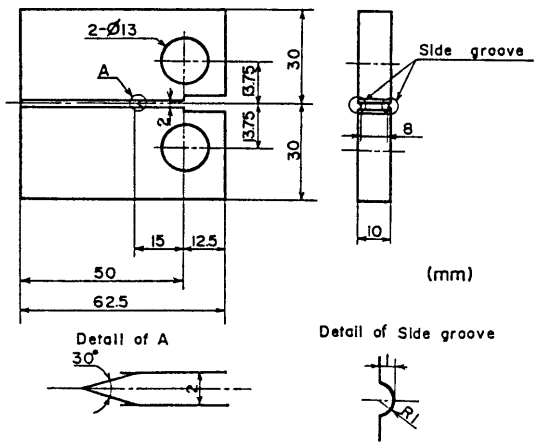

Fig. 1 Shape and dimensions of compact tension specimen used.

where the crack propagation rate da/dt is independent of the stress intensity factor, is formed over the maximum stress intensity factor, K_{max} of 22.5～38.0 MPam$^{1/2}$ with measured crack velocities of 0.9～1.0×10^{-9} m/sec. Therefore, the corrosion fatigue tests in this study were carried out at K_{max} above K_{ISCC}.

Figure 3 shows the experimental relationship between crack propagation rate, da/dN, and testing frequency, f. The frequency for the trapezoidal waveform is defined as $1/(t_c+t_h)$. There is clearly a trend that the fatigue crack propagation rate has a peak at a particular frequency value, f_{crit}, in the case of triangular waveform, and the effect of frequency on crack propagation rate is divided into two different regimes. That is, for $f \geq f_{crit}$, da/dN increases as f is decreased; on the other hand, da/dN decreases as f is decreased for $f \leq f_{crit}$. The critical test frequencies for this material are found to be over 0.05～0.1 Hz and dependent on the stress intensity range, ΔK. This behavior has been reported for some steels under the testing condition below K_{ISCC}[10]. It has been found that f_{crit} is 0.01～0.7 Hz and dependent on ΔK and solution temperature for such steels.

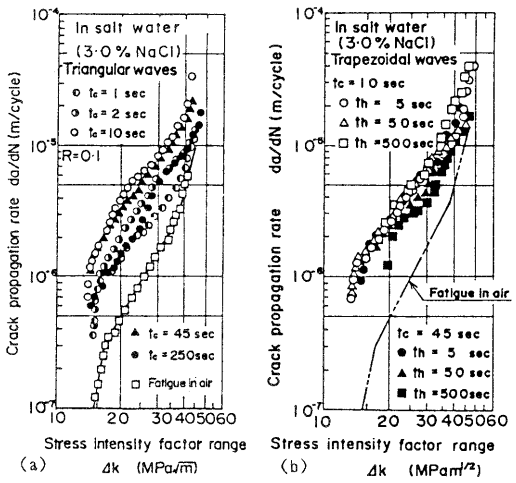

Fig. 2 Experimental relation between crack propagation rate da/dN and stress intensity range ΔK for A 7003-T 6 aluminum alloy under low-cycle fatigue in 3.0 % saline solution and laboratory air at $R=0.1$ and various frequencies: (a) Triangular waveform, (b) Trapezoidal waveform.

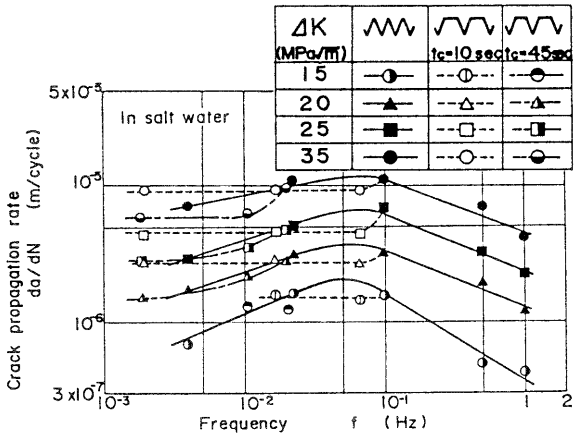

Fig. 3 The effect of loading frequency on da/dN for various ΔK values.

The relation between da/dN and f in the tests of trapezoidal waveform is different from the tendency of the triangular waveform. It is seen from Fig. 3 that da/dN of the trapezoidal waveform does not depend on frequency, and that no acceleration of da/dN occurs as the hold period is increased. This is attributable to such factors as dissolution at crack tip and change in the shape of the crack tip.

3.2 Behavior of crack closure

The relation between the crack opening ratio, $U(=(K_{max}-K_{op})/(K_{max}-K_{min}))$, and ΔK is shown in Fig. 4. The solid line in this figure represents the experimental results obtained from the fatigue test in air. The values of U obtained from the triangular waveform of $t_c=250$ s and the trapezoidal one with $t_h=500$ s are small as compared with those obtained in air because of the effect of corrosion products built up on crack wall. In the other experimental data, the crack opening stress diminishes with broadening crack tip by dissolution.

If the data of Fig. 3 are replotted in terms of the effective stress intensity factor $\Delta K_{eff}(=U\cdot\Delta K)$ instead of ΔK, as in Fig. 5, it is clear that da/dN in the trapezoidal waveform slightly increases with decreasing frequency; that is, increase of the stress hold time leads to environmental enhancement of the crack propagation rate.

3.3 The effect of an aqueous environment on fatigue crack propagation

For quantitative consideration of environmental

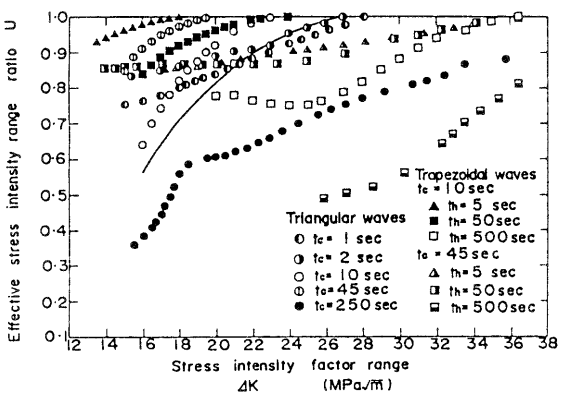

Fig. 4 Relation between crack opening ratio, U, and ΔK obtained from the triangular and trapezoidal waveforms.

effects on the fatigue crack propagation rate, Fig. 6 shows the experimental relationship between environmental acceleration factors $da/dN|_{CSCC}/da/dN|_{air}$ and $da/dN|_{CF}/da/dN|_{air}$ and loading frequency. Now, $da/dN|_{CSCC}$ and $da/dN|_{CF}$ are the crack propagation rates of trapezoidal and triangular wave loading in an aqueous environment, respectively. And $da/dN|_{air}$ is the crack propagation rate under testing at a frequency of 1 Hz in air. It is found from this figure that the maximum environmental acceleration factor corresponds to a particular frequency value in the case of the triangular waveform, which is the same as the f_{crit} mentioned before. Enhancement of corrosion fatigue crack propagation rates compared with those in an inert environment will disappear at very high frequencies above f_{crit} when there is insufficient time for environmental attack. On the other hand, the reduction in the environmental component of crack propagation controls the crack propagation rate at very low frequencies below f_{crit}. This type of behavior supports the idea proposed by Barsom[11] that corrosion fatigue crack propagation is an unstable equilibrium process due to a balance between two opposing mechanisms. The controlling mechanisms of crack propagation are considered to be consistent with a process of dissolution, passivation, filming over of the crack tip and/or actual changes in the crack tip profile. Formation and rupture of the passive film around the crack tip depend on strain rate, and the appearance of a fresh surface at the crack tip is an important control factor for dissolution.

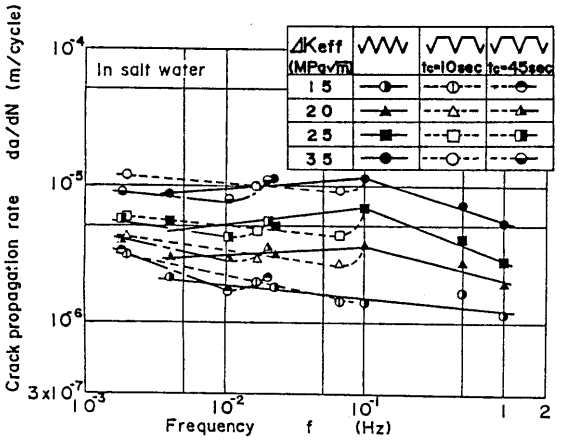

Fig. 5 The effect of loading frequency on da/dN for various values of effective stress intensity factor ΔK_{eff}.

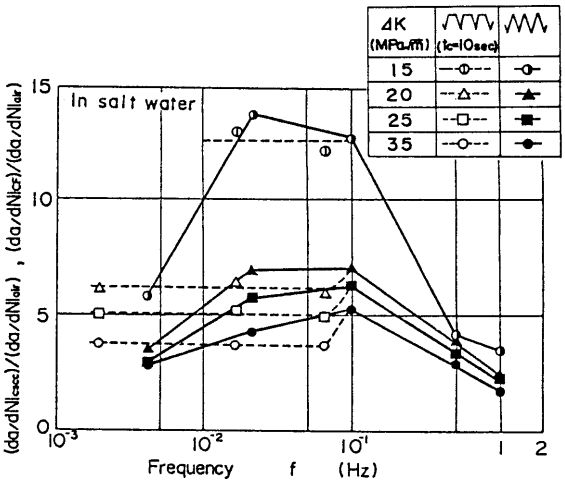

Fig. 6 Relation between environmental acceleration factor and loading frequency for the various values of ΔK in salt water.

The rate of loading or the strain rate controls the amount of environmental attack. The condition for sustained subcritical cracking in aqueous environments is that the slip/passive film rupture processes at the crack tip provide a supply of bare metal at a rate faster than that by which it is removed by the passivation reaction. The pumping action of a fatigue crack as it opens and closes is also an important control factor in environmental-assisted crack propagation because of the increase in reaction rates for liquid diffusion. The results obtained from the triangular waveform would be consistent with a process controlled by dissolution/passivation, but it is not possible to explain the behavior of crack propagation tested under the trapezoidal waveform with various stress hold periods.

The results presented in the preceding section suggest that the effect of dissolution at the crack tip on the fatigue crack propagation is two opposing mechanisms : One is enhancement of the fatigue crack propagation rate due to the dissolution. The other mechanism, which results in the reduction of the crack propagation rate, is affected by the shape of the crack tip. Crack extension and blunting or microbranching will exist together during the hold period. The retardation of crack propagation during stress cycling followed by holding occurs due to blunting or microbranching at the crack tip[9]. The formation of slip step and bare metal at the crack tip is a necessary condition for sustained subcritical cracking from the blunted or branched crack tip. In this case, stress cycling will be required, and the crack propagation rate may not be time dependent but cyclic. The existence of this behavior is proved by the evidence that the environmental acceleration factor in the trapezoidal wave did not depend on frequency, as shown in Fig. 6.

3.4 Change in shape of crack tip

It was suggested from the represented experimental results that the behavior of fatigue crack propaga-

tion under low cyclic loading is affected by the shape of the crack tip, which is changed due to dissolution. This has been pointed out by some investigators[4][7][9]. The stress intensity factor is usually determined by the method of fracture mechanics under the assumption of infinitesimally small curvature at the crack tip. The actual crack tip stress intensity factor developed under a corrosive environment must take into consideration the change in crack tip morphology and will consequently be less than the calculated stress intensity factor. But it is difficult to estimate directly the actual stress intensity factor and to observe the shape of the crack tip experimentally. The experimental relation between da/dN(or da/dt) and $\Delta K(K_{max})$ in subcritical crack growth differs depending on experimental conditions such as waveform, environment, and frequency, though this is reflected by the crack tip configuration. Under transient conditions, this is not the case. Change in atmosphere from a corrosive environment to an inert one may be achieved much more rapidly than the associated change in crack tip shape. The crack propagation rate immediately after such an environmental change is a function of the initial crack tip morphology associated with the inert environment. In this study, variation of the shape at the crack tip is investigated indirectly through the transition behavior of crack propagation from the test in a corrosive environment to that in air.

Figure 7 shows the experimental relationship between da/dN and ΔK obtained from the fatigue tests in air ($f=1$ Hz) after an arbitrary length of crack extension was made under the corrosion fatigue ($t_c=10$ s), trapezoidal wave ($t_c=10$ s, $t_h=50$ s) or SCC. It can be seen that the crack propagation rate is decreased just after switching from a corrosive environment to air. The degree of the retardation depends on the ΔK or K_{max} at the point of switching. These behaviors will reflect the appearance around crack tip. Therefore the actual stress intensity factor range ΔK^* was estimated by the method shown in Fig. 7, on the basis of the idea that the da/dN at the point of switching reflects the steady-state relation between da/dN and ΔK obtained from the fatigue test in air.

The estimated stress intensity factor range ΔK^* is shown in Fig. 8, plotted as open circles. The overall calculated difference between ΔK^* and ΔK is affected by the loading waveform in the corrosive environment and the ΔK (or K_{max} for SCC) at the point of switching. It can also be seen that ΔK^* coincides with ΔK in

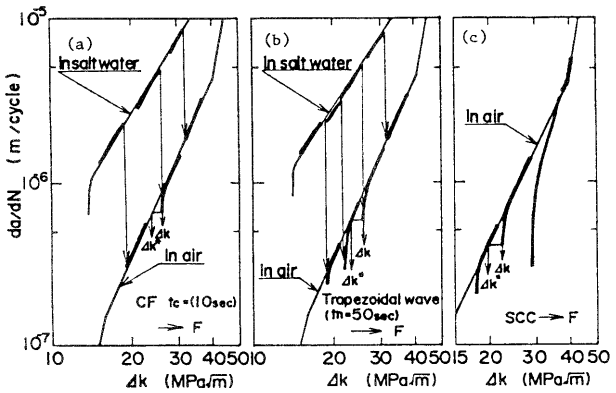

Fig. 7 Experimental relation between da/dN and ΔK under the transient conditions of change from a corrosive environment to air.

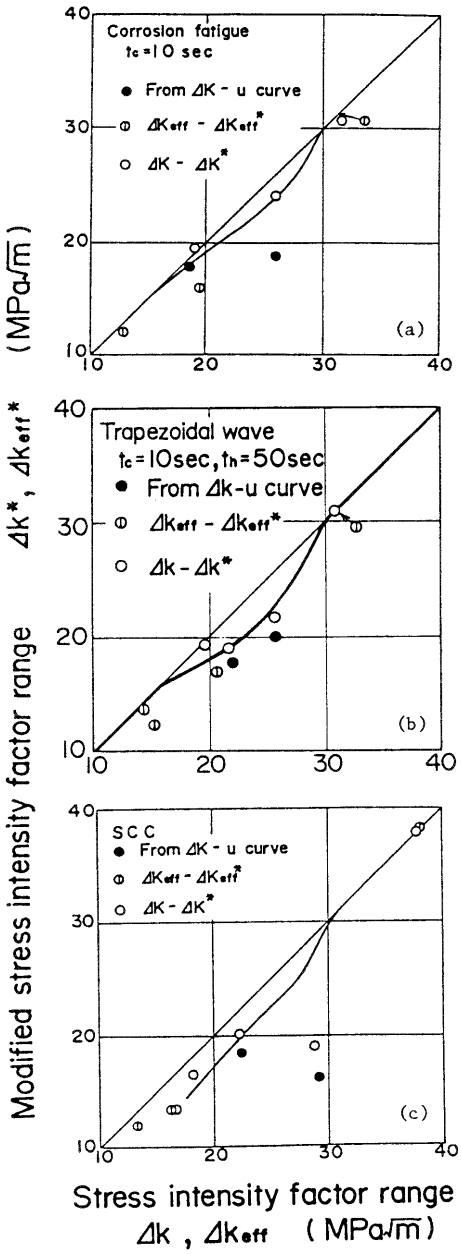

Fig. 8 Relation between estimated stress intensity range, ΔK^*, and ΔK.

the region of relatively low or high ΔK, and that change in the shape of the crack tip may be recorded in the medium range of ΔK. In the high ΔK range, crack propagation is controlled by mechanical damage as opposed to electrochemical damage, and crack blunting or microbranching decreases very rapidly. Therefore, there is not time for dissolution to take place before the crack tip passes any particular point in the material. Conversely, it appears that the optimal conditions for the stress corrosion process exist in the medium range of ΔK. Crack branching may substantially assist the damage caused by stress-assisted dissolution, and this is considered in the following section.

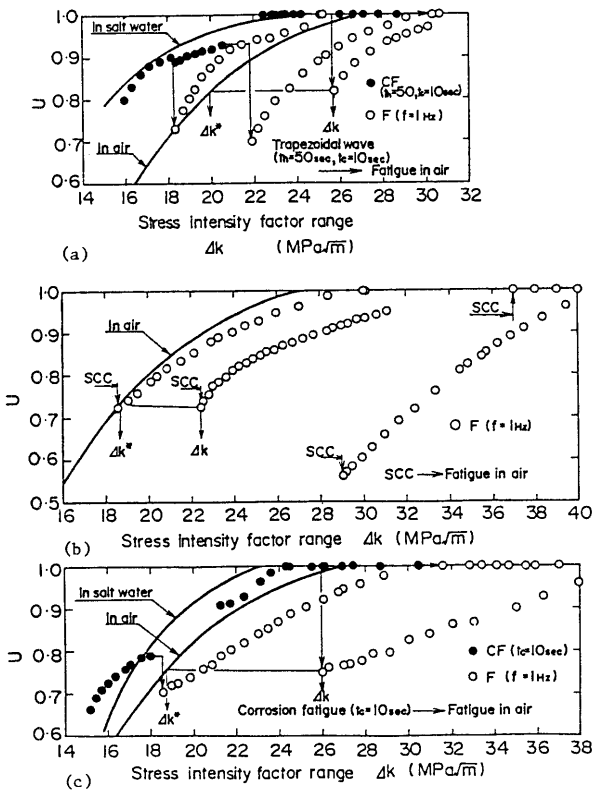

Fig. 9 Experimental relation between U and ΔK under the transient conditions of change from a corrosive environment to air.

Figure 9 shows the experimental relation between crack opening ratio U and ΔK obtained from the tests as shown in Fig. 7. It is obviously seen that the U value just after switching from the test in saline solution to that in air is decreased as compared with the $U-\Delta K$ relation in air, as indicated by the solid line. This behavior corresponds to the $da/dN-\Delta K$ relation in Fig. 7. Decrease of da/dN and U in air may result from the inhibition of mechanical fracture which occurs due to the action of microbranching and blunting with stress-assisted dissolution. In Fig. 8, the relation between ΔK^* and ΔK estimated from the results of the $U-\Delta K$ and $da/dN-\Delta K_{eff}$ diagram is also shown. Results estimated by different methods show good agreement with each other.

3.5 Crack branching

For discussion in detail of the change in the shape of the crack tip, the number and depth of secondary cracks formed under the fracture surface were measured using the specimens tested under various testing conditions. The central face of specimen thickness parallel to the direction of crack growth was polished for metallographic examination. The specimens were then examined under an optical microscope. Figure 10 is a typical example of secondary cracks. It can be observed from the pictures that there are a lot of secondary cracks which grow in a direction inclined 30~40 degrees from the fracture surface. The shape of secondary cracks depends upon the testing frequency. In the case of low frequency, cracks are blunted by dissolution and the fracture surface tends to be rough.

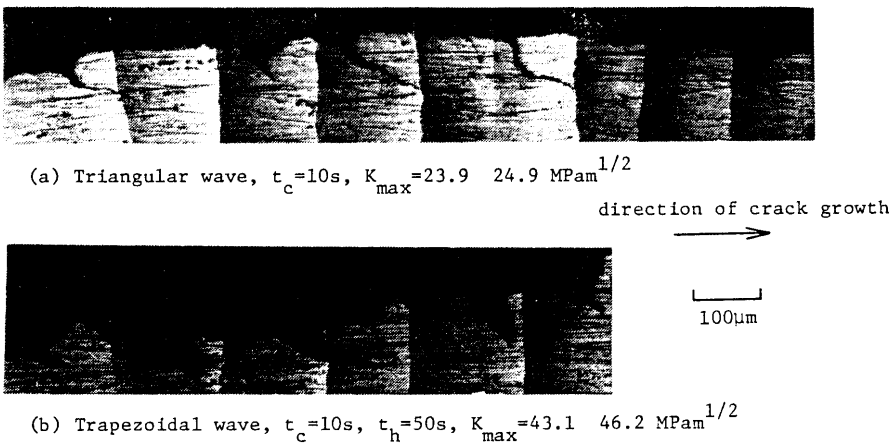

(a) Triangular wave, t_c=10s, K_{max}=23.9 24.9 MPam$^{1/2}$

(b) Trapezoidal wave, t_c=10s, t_h=50s, K_{max}=43.1 46.2 MPam$^{1/2}$

Fig. 10 Typical examples of secondary cracks formed under the fracture surface.

The length of secondary crack was defined as its depth perpendicular to fracture surface. Figure 11 shows the change in length of secondary cracks, p, and the number of secondary cracks per unit length, density ρ, accompanied by the maximum stress intensity factor K_{max}. It can be seen from the experimental results obtained under the various conditions of the tests that p and ρ tend to increase with K_{max} up to a particular value of K_{max} and after that decrease with increasing K_{max}. The value of K_{max} at which p is maximum is independent of the loading waveform and is 40 MPam$^{1/2}$. On the other hand, K_{max} at which ρ is the maximum is dependent on waveform and is small as compared with that for p.

Rhodes and Radon[12] have proposed the following equation for presumption of the actual stress intensity factor K^* when n close parallel cracks are applied:

$$K^*=\{(K^2/n)+6\pi p\sigma_y\}^{1/2} \quad (1)$$

where σ_y is the yield stress of the material and p is defined as the depth of exfoliation damage, which is a special type of stress corrosion. The secondary cracks will be formed intermittently at the main crack tip. It is difficult to evaluate how many secondary cracks have an influence on the main crack tip developed. In this investigation, p is treated as the depth of the secondary crack and n is assumed to take the following form:

$$n=1+\alpha\rho \quad (2)$$

where α is constant.

Figure 12 shows the relation between ΔK^* and ΔK calculated by means of Eqs.(1) and (2) using the experimental values of p and ρ obtained from the test of trapezoidal waveform with hold period of $t_h=50$ s ($t_c=10$ s). In this figure, α is an arbitrary parameter and the relation between ΔK^* and ΔK is determined by the selection of α, which may be a function of crack morphology and cannot be measured directly. Discussion of the physical meaning of α is in progress and will be reported separately in the near

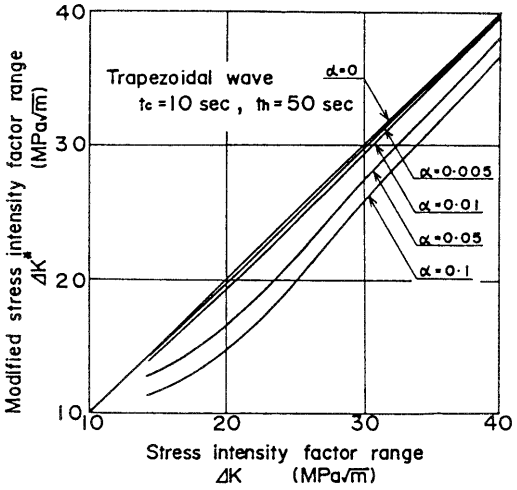

Fig. 12 Calculated relationship between ΔK^* and ΔK for various values of α.

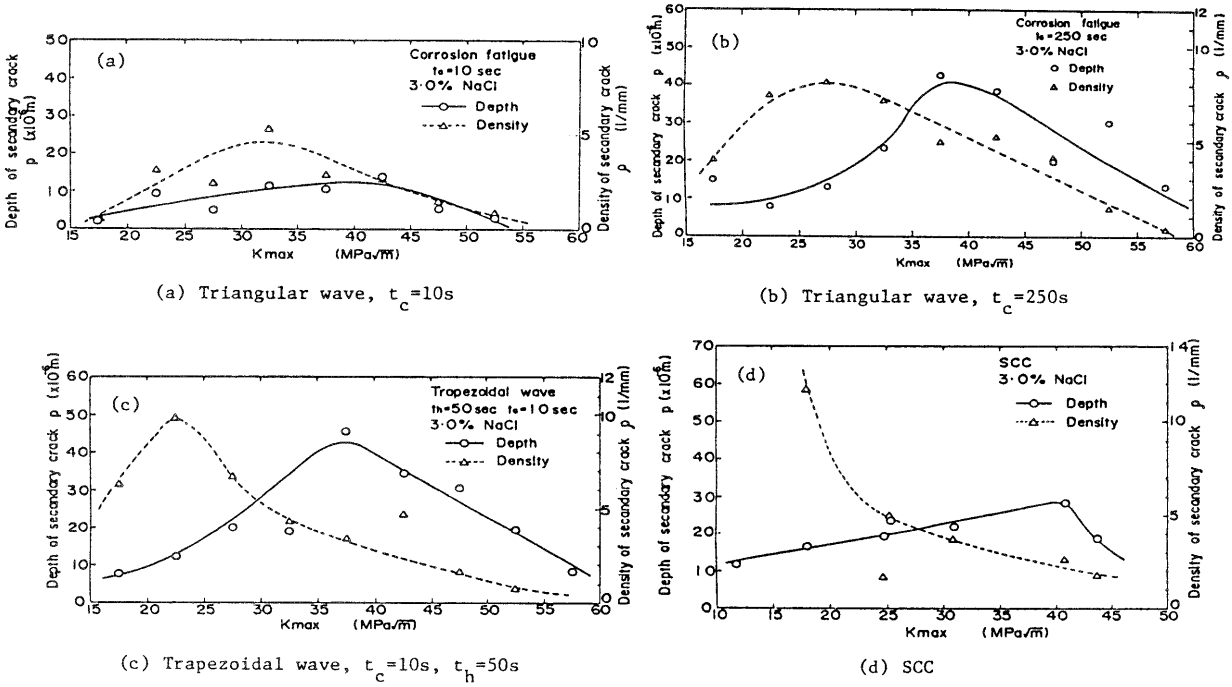

(a) Triangular wave, t_c=10s

(b) Triangular wave, t_c=250s

(c) Trapezoidal wave, t_c=10s, t_h=50s

(d) SCC

Fig. 11 Experimental relation between depth and density of secondary cracks and K_{max} under the various testing waveforms.

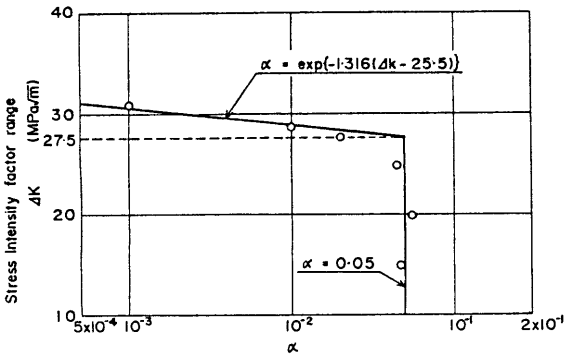

Fig. 13 Relation between value of α taken during crack propagation and ΔK under the test of trapezoidal waveform with $t_h=50$ s.

future. The value of α taken during crack propagation can be obtained from a comparison between the calculated $\Delta K^*-\Delta K$ relation and the experimental data, as shown in Fig. 8. Figure 13 shows the relation between α and ΔK, and the following equation is glven:

$$\left.\begin{aligned} &\Delta K>27.5\ \mathrm{MPam^{1/2}}\\ &\quad \alpha=\exp\{-1.316(\Delta K-25.5)\}\\ &\Delta K<27.5\ \mathrm{MPam^{1/2}}\\ &\quad \alpha=0.05 \end{aligned}\right\} \qquad (3)$$

Using Eqs.(1)～(3), the $\Delta K^*-\Delta K$ relation is obtained for the various conditions of the tests and the calculated results are indicated by the solid line in Fig. 9. It is found that the calculated results of stress intensity factor range ΔK^* which take the distribution and length of secondary cracks into consideration are in good agreement with those estimated from the experiments.

4. Conclusions

(1) The effect of cyclic frequency, f, on crack propagation rates in the triangular waveform was found to be exemplified by two different regimes. One has a positive dependency on frequency below a critical frequency, f_{crit}, at which maximum environmental attack occurs in terms of da/dN, and the other is negative above f_{crit}.

(2) The crack propagation rate, da/dN, under the tests of trapezoidal waveform with stress hold periods in $f\leq f_{crit}$ did not depend on testing frequency for various values of ΔK.

(3) Crack tip morphology was investigated through the transition behavior of crack propagation rate from the tests in a corrosive environment to those in air. The actual stress intensity factor was less than the calculated one because of blunting or microbranching at the crack tip by dissolution.

(4) On the basis of experimental measurement, the length and density of secondary cracks formed under the fracture surface were found to be dependent on K_{max} and loading waveform and closely related to the sensitivity to stress corrosion cracking of the material.

(5) Crack propagation under low cyclic corrosion fatigue is controlled by two opposing mechanisms. One is enhancement due to the stress-assisted dissolution; the other one, which results in reduction of crack propagation, is affected by blunting or microbranching at the crack tip. It is necessary to take into account the crack tip morphology for modelling of crack propagation behavior under low-cycle corrosion fatigue.

Acknowledgements

The authors would like to thank Mr. Hideo Maeda of Sumitomo Aluminum Seiren Co. Ltd. for kindly supplying of A 7003-T 6 and Mr. Toshinobu Tomosaka of the Department of Mechanical Engineering, Toyama University, for his very able assistance with the experiments described in this paper.

References

(1) Endo, K. and Komai, K., Low-Cycle Corrosion Fatigue of Aluminum Alloy, J. Soc. Mater. Sci., Jpn., (in Japanese), Vol. 14, No. 145(1965), p. 827.

(2) Kawai, S. and Koibuchi, K., Effects of Stress Waveforms and Frequencies on Fatigue Crack Growth in 3% NaCl Solution, Trans. Jpn. Soc. Mech. Eng., (in Japanese), Vol. 44, No. 382(1978), p. 1789.

(3) Yokobori, T., Yokobori,T and Takasu, N., Stress Hold Time and Stress Rising Time Effect on Corrosion Fatigue Crack Growth Rate, Trans. Jpn. Soc. Mech. Eng., (in Japanese), Vol. 52, No. 477(1986), p. 1232.

(4) Endo, K., Komai, K. and Suzuki, Y., Influences of Stress Cycle Frequency on Propagation of Corrosion Fatigue Cracks, Trans. Jpn. Soc. Mech. Eng., (in Japanese), Vol. 40, No. 333 (1974), p. 1262.

(5) Wei, R. P. and Landes, J. D., Correlation between Sustained-Load and Fatigue Crack Growth in High-Strength Steels, Mater. & Stds., Vol. 9, No. 1(1969), p. 25.

(6) Austen, I. M. and Walker, E. F., Quantitative Understanding of the Effects of Mechanical and Environmental Variables on Corrosion Fatigue Crack Growth Behaviour, Proc. IMechE, London, Paper C 98/77(1977).

(7) Rhodes, D., Musuva, J. K. and Radon, J. C., The Significance of Stress Corrosion Cracking in Corrosion Fatigue Crack Growth Studies, Eng. Frac. Mech., Vol. 15, No. 3-4(1981), p. 407.

(8) Shiozawa, K., Cyclic Stress Corrosion Cracking of Aluminum Alloy, J. Soc. Mater. Sci., Jpn.,(in

Japanese), Vol. 28, No. 314(1979), p. 1122.
(9) Shiozawa, K., Crack Growth during Cyclic Stress Corrosion Cracking in Aluminum Alloy, J. Soc. Mater. Sci., Jpn., (in Japanese), Vol. 33, No. 365(1984), p. 172.
(10) Atkinson, J. D. and Lindley, T. C., The Effect of Frequency and Temperature on Environmentally Assisted Fatigue Crack Growth Below K_{Iscc} in Steel, Proc. I. Mech. E., London, Paper C 106/77(1977).
(11) Barsom, J. M., Corrosion Fatigue Crack Propagation Below K_{Iscc}, Eng. Fract. Mech., Vol. 3,(1971), p. 15.
(12) Rhodes, D. and Radon, J. C., Fracture Analysis of Exfoliation in an Aluminum Alloy, Eng. Fract. Mech., Vol. 10(1978), p. 843.